

# Tuning Optimization Approaches for Digitally Controlled Tunable Filters

Yarkin YIGIT

Department of Electrical and Electronics Engineering  
Gebze Technical University  
ASELSAN A.S.  
Ankara, Turkey  
yyigit@aselsan.com.tr

Erdem YAZGAN

Department of Electrical and Electronics Engineering  
TED University  
Ankara, Turkey  
erdem.yazgan@tedu.edu.tr

**Abstract**—Increase of data and voice communications imposed the demand for wide band systems and technologies. In this scope reconfigurable/tunable microwave (MW) filters were widely employed in the radio frequency (RF) receivers, which are the integral components for wireless, 5G, radar, and satellite communication systems. They are used in pre-selection and intermediate frequency (IF) bandpass filters to eliminate undesired signals in receivers. Various technologies and materials were used to develop such filters such as RF MEMS, semiconductor diodes, and ferroelectrics. In this manuscript, significance and comparison of tunable filter technologies are explained and their three different control levels (tuning element, resonator, and filter) are discussed. We also elaborate on the open and closed loop tuning methods and optimization techniques. Finally, we present the results of a control algorithm, which we developed to drive and optimize the frequency range of an yttrium-iron-garnet (YIG) filter.

**Keywords**—Tunable filter, receiver, filter frequency control, YIG filter.

## I. INTRODUCTION

The operating frequency bands for the cellular systems have been increased to over 40 bands due to the increasing demand in the channel capacity of the mobile communication networks. Long term evolution (LTE) and especially future 5G infrastructures are the technologies to increase the communication speed, latency, and bandwidth. Filters are among the most significant components, since they are widely used in transceivers, software defined radios, and cognitive radios. The solution to the multiband and multimode communication to achieve smaller size and lower cost is to adapt reconfigurable radio frequency (RF) components for these systems. Reconfigurable filters make microwave transceivers adaptable to multiple bands operations. They can replace some traditional filters owing to their reconfigurable center frequency and bandwidth. They suggest compactness, wide tuning range, more functionality, better channel selectivity, reduced size, and lower weight. In addition, while they eliminate unwanted signals, low-noise amplifier (LNA) linearity becomes better and power consumption of analog-to-digital converter (ADC) may be reduced in receivers. Microwave tunable filters can be divided in two groups as discretely and continuously tunable filters. Filter topologies presenting a discrete tuning generally use PIN diodes or MEMS

switches. On the other hand, filter topologies using varactor diodes, MEMS capacitors, ferroelectric materials or ferromagnetic materials are frequently used to obtain a continuously tunable device. Depending on the application, combination of both tuning techniques may be possible.

For discretely tunable filters, PIN diodes are frequently used to produce reconfigurable discrete states on filter response. This technique has been used to implement a few switchable bandstop or bandpass filters. These filters have been implemented to provide the same fractional bandwidth at defined center frequencies [1, 2]. MEMS switches are used to produce discrete tuning of reconfigurable parameters. These switches can be capacitive or direct contact type, which are applicable for low frequency and high frequency applications, respectively [3].

For continuously tunable filters, varactors are the typically used components, which offer high tuning speeds as well as low power consumption. However, they suffer from low quality factor (Q-factor) and power handling issues. Varactor diodes generate unwanted distortions when large input power present since they are originally non-linear devices. RF MEMS varactor technology have good compatibility with the processes used in semiconductor industry as well as they low power consumption compared to the solid state devices. Moreover, they exhibit linear transmission at low signal signal solution.[4].

Ferroelectric and ferromagnetic filters are also continuously tunable filters, of which permittivity values proportional to externally applied electric field. Barium-strontium-titanate oxides (BST) [5] and yttrium-iron-garnet (YIG) are among the most common material systems addressing ferrite technologies. Having a high Q, BST material is a good candidate for tunable components. Their harmonic performance and suppressions in stop-band are better than those of GaAs varactors. This comparison is provided in reference [6]. In addition, tunable filters using ferromagnetic materials like yttrium-iron-garnet (YIG) have high Q-factors as well and render resonators with high power handling capabilities and high power consumption rates [7,8]. However, these filters require very precise material growth and fabrication technologies which lead to high costs.

Another drawback may be the low tuning speed along with a complex tuning mechanism [7].

Table 1. Comparison of different tunable filter technologies.

| Tuning Method       | Mechanical | YIG        | GaAs Varactor | RF MEMS   | BST Thin Film |
|---------------------|------------|------------|---------------|-----------|---------------|
| Tuning range        | 5:1        | Multi oct. | 3:1           | < 2:1     | 2 - 3:1       |
| Q                   | > 1000     | > 500      | 10 - 40       | High      | 20 - 100      |
| Insertion Loss (dB) | 0.5 - 2.5  | 3 - 8      | 2 - 10        | 2 - 8     | 3 - 8         |
| Tuning Speed        | Millisec.  | Millisec.  | Nanosec.      | Microsec. | Microsec.     |
| Power Capability    | High       | 2 W        | ~ mW          | 1 - 2 W   | ~ mW          |

In a communication system, industry generally requires a much narrower band than the entire bandwidth of the system. For example in ultra high frequency (UHF) tactical and cognitive radios, a good performance is achieved with only 25 kHz bandwidth. Hence the ideal condition is to assign 25 kHz for a voice channel. However, practically it is almost impossible to design such a filter. A more feasible solution may be adopted through designing the filter response near 10 MHz bandwidth. On the choice of technology the comparison given in Table 1 may be a starting point for a desired application. The designer must consider cost, power consumption, size, performance and operating frequency. For example, when the tuning speed is the primary design criterion, GaAs varactor diode or BST may be the correct technology, on the other hand when narrow bandwidth and wide tuning range are the favored specifications, YIG filters may be the optimum solution.

## II. CONTROL LEVELS AND MEASUREMENT METHODS OF TUNABLE FILTERS

In this part, we will discuss three levels of control for tunable filters consist of device level, resonator level, and filter level tuning operations. We will also describe the methods of measurements briefly.

Device-level control is basically to control the tuning element itself and meet the certain bandwidth and center frequency requirement. Resonator-based control involves tuning each resonator to a precise resonant frequency. For example, lumped V/UHF narrow band tunable filter is designed as described in reference [6]. The advantage of this technique is that the state measurement is performed at a frequency outside the operating band of filter.

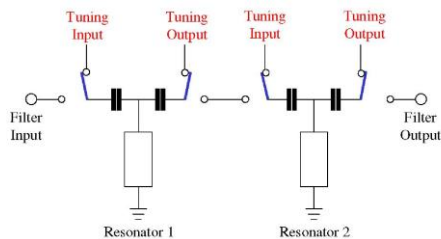


Fig.1. Resonator based tuning [8]

As a third level tuning operation, filter-level control is tuning both resonators and coupling parameters together. By tuning the resonance frequency of the resonators, the center frequency of

the filter is adjusted while adjusting the coupling that affects the bandwidth of the filter. Robotic computer aided tuning also known as RoboCAT is an example of filter level tuning operation [9].

Measurement methods of the tunable filters are described in three categories as follows: As a first method, the single-frequency reference signal is employed by using a single reference tone to tune each resonator for maximum response at the center frequency. As a second method, multi-frequency reference signal is employed using a multi-tone signal to reduce the number of necessary measurements. Third and final method may be the swept-frequency signal technique, which involves a series of measurements to be performed to determine the response of the filter over a frequency range [10]. In our work, we used the swept frequency signal technique using a network analyzer to obtain more accurate results.

Post production tuning is critical and significant to achieve desired response from the filter. There are three main classes of tuning algorithms for traditional filters. These are sequential techniques which are time domain tuning and group delay methods, fuzzy logic based on artificial intelligence, and deterministic models and space mapping tuning model through coupling matrix from s-parameters to find error matrix [10,11]. Parameter extraction, fuzzy logic, and sequential techniques are used for fixed filters instead of tunable filters as a post production tuning, because of varying resonator model complexity. For tunable filters, look-up table and optimization methods are used as a tuning algorithm to obtain stable filter responses.

According to look-up table method, these filters have different responses for applied voltage levels which are in the component specification limits. In the frequency domain, the filter is pre-characterized and the tuning states are pre-configured into the memory of the controller with respect to electrical bias before using in a upper level module. In the optimization method, a goal function is established and an iterative algorithm is employed to find the optimal tuning voltages in order to minimize the value of the objective function [12].

After designing, production and tuning process of tunable filters, they are operated in optimum region but it is difficult to observe and measure results in time. They are controlled through the same control signals and initial values are assumed to be right. However, tuning errors including hysteresis especially for YIG filters, non-linearity, frequency drift over temperature, and aging of the components can not be compensated. Necessary corrections may be applied within the open loop modality for which the tuning must be done from the beginning.

In order to correct these errors, closed loop method is used as well. This approach utilizes the transmitter carrier as a reference signal and uses its reflection phase change from the notch filter to tune the notch filter frequency. Since the  $S_{21}$  of the notch filter exhibits a  $180^\circ$  phase jump at its notch frequency, the phase information of reflected reference signal must be used. Because of  $S_{11}$  reflection phase behavior versus frequency is continuous and magnitude is very high.

### III. LOOK-UP TABLE METHOD FOR OPEN-LOOP TUNING

The scope of this manuscript is limited with the open loop tuning method in order to optimize the tunable filters which have different topologies and different operating frequencies. For this purpose, a look up table and optimization software were developed for 2-18 GHz YIG tunable filters.

YIG-based filters are excellent for military applications because of their low loss, wideband tuning, and excellent linearity. However, hysteresis effect due to the magnetic properties of YIG material should be compensated. In addition, since the tuning of this material is a highly tedious operation, a very stable digital to analog converters (DAC) must be used to prohibit voltage variations on the filter. In our work, we developed a software-based compensation method using the open-loop technique in order to compensate hysteresis and aging errors.



Fig. 2. YIG filter measurement setup.

YIG filter tuning setup consists of a voltage controller fed by a voltage source and a digital controller, a PNA and a PC. The setup was shown in Fig. 2. Measurements were taken in different driving voltage levels using swept frequency signal method.

Calibration table was built and its software was developed in Visual Studio.NET platform. According to control interface shown in Fig. 3 power sources and PNA connections can be made both manual and automatic. Also integral filter driver can be controlled by viperboard which is managed by the operator. Also user can send commands as a 12 bit array manually to verify the desired condition. For loading of the data, initially latch triggered level must be low and with the rising of this level, information is transferred to voltage driver.

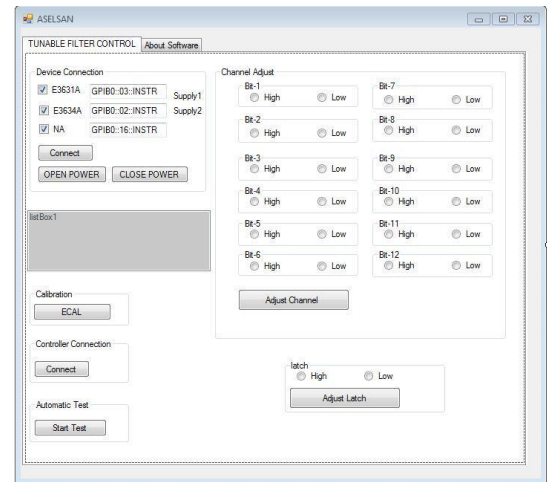


Fig.3. YIG filter control interface.

Measurement was performed for 12 bit TTL input compatible with latch in 4096 steps. For every step, filter response, i.e.,  $S_{21}$ ,  $S_{11}$ , 3 dB bandwidth, and center frequency have been measured with 3.9 MHz resolution.  $S_{21}$  and  $S_{11}$  parameters of the filter are shown in Fig. 4 and Fig.5, respectively, for different digital biases.  $S_{21}$  notch amplitudes can be varied from -5 dB to -78 dB (see Fig.4) because of high quality factor (Q factor) of YIG resonators and existing excellent couplings between of them. Also wide tuning range is based on same property. Reflection signals can be varied from -1.4 dB to -6.2 dB at the notch frequencies, where suppressions are extremely high (see Fig.5).

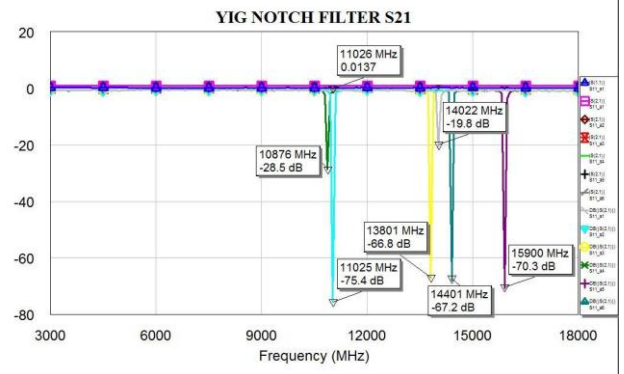


Fig.4. YIG 2-18 Notch Filter  $S_{21}$

Selectivity and isolation of the filter depend on the number of resonators in the filter. In this work, we used a filter with 4 stages. Changes in the coupling coefficients were observed within the frequency range of interest as well as altering of the bandwidth. In addition, 3 dB bandwidth and amplitude, off resonance spurious (ORS) and rejection levels which are difference between 3 dB amplitude level and strongest spurious signal are measured from 2 GHz to 18 GHz with 3.9 Mhz resolution.

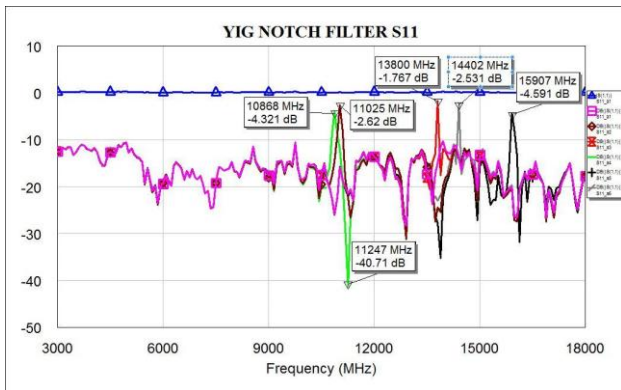


Fig.5. YIG 2-18 Notch Filter S11

Since showing all responses in same graph is not comprehensible, results are presented for 8 different voltage levels. They were recorded in the calibration table as shown in Fig. 6. According to this table, each bias voltage corresponds to a filter center frequency. After a certain time, it is expected that these frequency and bias pair will not match to each other. So the table must be updated frequently. All performance values can be seen in the table, and it gives a guidance to the operator about the in-spec or out-of-spec filters. For a proper notch filter, suppression values should be lower than -10 dBm. In addition to that, the spurious signals should be lower than 0.8 dBm as well as 3 dB bandwidth should be narrower than 50 MHz to generate a successful tuning using the calibration table.

| YIG FILTER CALIBRATION TABLE |                        |              |                      |              |              |         |         |                 |
|------------------------------|------------------------|--------------|----------------------|--------------|--------------|---------|---------|-----------------|
| Digital (Decimal)            | Center Frequency (MHz) | S21 Amp (dB) | 3 dB Bandwidth (MHz) | 3 dB AMP(dB) | S11 Amp (dB) | LHS ORS | RHS ORS | Rejection Level |
| 2064                         | 10676.12               | -6.10        | 106.444              | -6.296       | -6.289       | -0.487  | -0.439  | -5.81           |
| 2154                         | 11028.34               | -10.27       | 56.739               | -8.736       | -8.754       | -0.427  | -0.655  | -8.31           |
| 2856                         | 13801.42               | -33.33       | 14.611               | -7.992       | -7.804       | -0.431  | -0.764  | -7.56           |
| 2912                         | 14022.61               | -67.83       | 6.822                | -1.133       | -0.979       | -0.431  | -0.537  | -0.70           |
| 3008                         | 14401.77               | -12.20       | 44.062               | -3.877       | -3.896       | -0.435  | -0.655  | -3.44           |
| 3362                         | 15800.32               | -14.08       | 36.648               | -10.987      | -11.030      | -0.435  | -0.572  | -10.55          |
| 3524                         | 16439.21               | -67.50       | 6.831                | -2.283       | -2.225       | -0.425  | -0.429  | -1.86           |
| 3669                         | 17012.11               | -5.44        | 156.628              | -5.230       | -5.648       | -0.425  | -0.428  | -4.81           |

Fig. 6. 2-18 YIG notch filter calibration table.

Additionally, the values of tuning parameters measured initially and afterwards can be stored in the same data file using the developed software to calculate hysteresis and linearity.

\*LHS ORS:Off resonance spurious signals at left hand side of the center frequency  
 \*RHS ORS:Off resonance spurious signals at right hand side of the center frequency

| YIG FILTER CALIBRATION TABLE (NOW) |                        |              |              | FILTER CALIBRATION TABLE (BEFO) |              |              | HYSTERESIS (MHz) | LINEARITY CALCULATION |
|------------------------------------|------------------------|--------------|--------------|---------------------------------|--------------|--------------|------------------|-----------------------|
| Digital (Decimal)                  | Center Frequency (MHz) | S21 Amp (dB) | S11 Amp (dB) | Center Frequency (MHz)          | S21 Amp (dB) | S11 Amp (dB) |                  |                       |
| 2064                               | 10676.12               | -6.10        | -6.289       | 10756.12                        | -6.10        | -6.289       | -80.00           | FAIL                  |
| 2154                               | 11028.34               | -10.27       | -8.754       | 11115.34                        | -10.27       | -8.754       | -87.00           | FAIL                  |
| 2856                               | 13801.42               | -33.33       | -7.804       | 13911.42                        | -33.33       | -7.804       | -110.00          | FAIL                  |
| 2912                               | 14022.61               | -67.83       | -0.979       | 14109.61                        | -67.83       | -0.979       | -87.00           | FAIL                  |
| 3008                               | 14401.77               | -12.20       | -3.896       | 14510.77                        | -12.20       | -3.896       | -109.00          | FAIL                  |
| 3362                               | 15800.32               | -14.08       | -11.030      | 15902.32                        | -14.08       | -11.030      | -102.00          | FAIL                  |
| 3524                               | 16439.21               | -67.50       | -2.225       | 16510.21                        | -67.50       | -2.225       | -71.00           | FAIL                  |
| 3669                               | 17012.11               | -5.44        | -5.648       | 17101.11                        | -5.44        | -5.648       | -89.00           | PASS                  |

Fig. 7. YIG filter hysteresis and linearization table.

Hysteresis means different tuned frequency of filter at the same coil current and it is caused by an unstable magnetization. Frequency shifts over time can be seen clearly in calibration table. Linearity tells us whether stability of the filter has deteriorated or not over time. In order to find linearity of the notch filter response, center frequencies for each digital bias have been analyzed for each sequential step and this limit is determined to be 3.95 MHz.  $F_1$  and  $F_2$  are sequential filter center frequencies for related bias values in Eq. (1) and linearity ratio is accepted in 5 % error tolerance. It is seen as "fail" in Fig. 7 since the measurements were not taken sequentially.

$$Linearity = \frac{F_2 - F_1}{3.95}. \quad Eq. (1)$$

The altered notch filter center frequency can be determined with 3.90 MHz resolution and digital data can be updated with respect to the calibration table for up-to-date tuned utilization of the filter. Thus, filters can be operated with the accurate voltage and center frequency pair information.

#### IV. CONCLUSION

Significance of digital tunable RF filters and their design technologies presented. Also tuning algorithm methods for traditional and tunable filters revealed, in addition open loop and closed loop control methodologies were explained. Open loop method was used to optimize 2-18 GHz YIG tunable notch filter with deriving of calibration table via our design software. It was presented that tuning errors which are hysteresis, non-linearity and aging of components were corrected with calibration software algorithm based compensation method by comparing the previous and current measurements.

As the result it is shown that when closed loop technologies are not used, open loop tunable filter performance can be optimized via calibration software.

Finally, radar warning and electronic intelligence (ELINT) systems or rejecting signals in commercial test equipment measurement set-ups which cover tunable filters, work more stable and efficient.

This work was supported by ASELSAN Inc.

#### References

- [1] Brito-Brito, Z.; Llamas-Garro, I.; Pradell, L. & Corona-Chavez, A. (2008). Microstrip Switchable Bandstop Filter using PIN Diodes with Precise Frequency and Bandwidth Control, *Proceedings of 38th European Microwave Conference*, pp. 126 –129, Amsterdam, The Netherlands, 27-31 Oct. 2008.
- [2] Brito-Brito, Z.; Llamas-Garro, I. & Pradell, L. (2009)b. Precise Frequency and Bandwidth Control of Microstrip Switchable Bandstop Filters, *Microwave and Optical Technology Letters*, Vol. 51, No. 11, November 2009, pp 2573-2578.
- [3] Ocera, A.; Farinelli, P.; Mezzanotte, P.; Sorrentino, R.; Margesin, B. & Giacomozzi, F. (2006). A Novel MEMS-Tunable Hairpin Line Filter on

- Silicon Substrate, *Proceedings of 36<sup>th</sup> European Microwave Conference*, pp. 803 – 806, 10-15 Sep. 2006.
- [4] Entesari, K. & Rebeiz, G., M. (2005)a. A differential 4-bit 6.5-10 GHz RF MEMS tunable filter, *IEEE Transactions on Microwave Theory and Techniques*, Vol. 53, No. 3, Part 2, Mar.2005; pp. 1103 – 1110.
- [5] Courreges, S.; Li, Y.; Zhao, Z.; Choi, K.; Hunt, A. & Papapolymerou, J. (2009). A Low Loss XBand Quasi-Elliptic Ferroelectric Tunable Filter, *IEEE Microwave and Wireless Components Letters*, Vol. 19, No. 4, Apr. 2009, pp. 203 – 205.
- [6] Yarkin Yigit and Erdem Yazgan. Comparison of Ferroelectric and Varactor Tunable Filters Controlled By DAC, 2015 *IEEE 15<sup>th</sup> Mediterranean Microwave Symposium (MMS)*.30 Nov-2 Dec 2015
- [7] Carter, P., S. (1961). Magnetically Tunable Microwave Filters Using Single Crystal Yttrium Iron Garnet Resonators, *IRE Transactions on Microwave Theory and Techniques*, Vol.9, pp 252-260
- [8] G. Tsuzuki, M. Hernandez, E. M. Prophet, S. Jimenez, and B. A. Willemsen, Ultra-selective constant-bandwidth electromechanically tunable HTS filters, *Proc. IEEE MTT-S Int. Microw. Symp. Digest*, 1-16 June 2006, pp. 693-696.
- [9] M. Yu and W.-C. Tang (Invited), A fully automated filter tuning robot for wireless base station diplexers, *Workshop: Computer Aided Filter Tuning, IEEE Int.*
- [10] Microw. Symp., Philadelphia, PA., June 8{13 2003.
- [11] T. C. Lee and J. Y. Park, 2009. Compact PCB embedded tunable filter for UHF TV broadcasting, *Microwave Symposium Digest*, 2009. MTT '09. IEEE MTT-S International, 7-12 June, pp. 505-508.
- [12] A. Jaschke, M. Tessema, M. Schuhler and R. Wansch, 2012. *Digitally tunable bandpass filter for cognitive radio applications, Computer Aided Modeling and Design of Communication Links and Networks (CAMAD)*, 2012 IEEE 17th International Workshop on, 17-19 Sept., pp. 338-342.